

Color-tuned neurons are spatially clustered according to color preference within alert macaque posterior inferior temporal cortex

Bevil R. Conway^{a,1} and Doris Y. Tsao^b

^aNeuroscience Program, Wellesley College, Wellesley, MA 02481; and ^bDivision of Biology, Caltech, Pasadena, CA 91125

Edited by David H. Hubel, Harvard Medical School, Boston, MA, and approved August 21, 2009 (received for review October 29, 2008)

Large islands of extrastriate cortex that are enriched for color-tuned neurons have recently been described in alert macaque using a combination of functional magnetic resonance imaging (fMRI) and single-unit recording. These millimeter-sized islands, dubbed “globs,” are scattered throughout the posterior inferior temporal cortex (PIT), a swath of brain anterior to area V3, including areas V4, PITd, and posterior TEO. We investigated the micro-organization of neurons within the globs. We used fMRI to identify the globs and then used MRI-guided microelectrodes to test the color properties of single glob cells. We used color stimuli that sample the CIELUV perceptual color space at regular intervals to test the color tuning of single units, and make two observations. First, color-tuned neurons of various color preferences were found within single globs. Second, adjacent glob cells tended to have the same color tuning, demonstrating that glob cells are clustered by color preference and suggesting that they are arranged in color columns. Neurons separated by 50 μm , measured parallel to the cortical sheet, had more similar color tuning than neurons separated by 100 μm , suggesting that the scale of the color columns is <100 μm . These results show that color-tuned neurons in PIT are organized by color preference on a finer scale than the scale of single globs. Moreover, the color preferences of neurons recorded sequentially along a given electrode penetration shifted gradually in many penetrations, suggesting that the color columns are arranged according to a chromotopic map reflecting perceptual color space.

column | cone | functional MRI | functional architecture | primate

Cells sharing similar receptive-field properties often are arranged according to columns within the cerebral cortex. Columns can be defined as “clusters of cells sharing common receptive field properties” (1). Cells are clustered by orientation preference within the primary visual cortex (V1) (2), by direction tuning within extrastriate area MT (3), and by disparity tuning within extrastriate area V3 (4). As Hubel and Wiesel (5) and Barlow (6) have argued, clustering cells by receptive-field properties like motion or depth would facilitate the computations required to generate linking features used to associate related parts of an image. The particular linking features would dictate the nature of the columns and perhaps the arrangement of the columns within the cortex. Barlow hypothesized that the cortex responsible for color would contain color columns, “thus making it easy to establish links between regions of the same color in the original image” (6).

Large (millimeter-sized) color modules have been found downstream of V2 using functional MRI (fMRI) and confirmed using single-unit recording (7). We refer to these modules as “globs,” to distinguish them from other sorts of modules found in other regions of the cortex (e.g., face patches, inferior temporal feature columns). The term “glob” has the additional advantage of drawing an analogy with the cytochrome-oxidase blobs of V1, an earlier stage in the hierarchical elaboration of color (8). The globs are millimeter-sized and scattered throughout the posterior inferior temporal cortex—a swath of brain also

referred to as the V4 complex (9). The scale of the globs is similar to the size of the patches of labeled cells found in the posterior inferior temporal cortex (PIT) following anterograde injections of tracer into the subcompartments of V2 (cytochrome-oxidase thin stripes) that are especially concerned with encoding color (10–12). fMRI-guided single-unit recording targeting the globs reveals that the vast majority of glob cells are color-tuned (7). The color tuning of this population strongly suggests its involvement in color perception (13, 14), but it remains unknown if the cells are organized within the globs, as might be expected following Barlow’s hypothesis. Some findings have suggested that color-tuned neurons in the V4 complex are clustered by color preference (15), although the notion that the V4 complex is specialized for color remains controversial (16, 17). Here we examine the functional organization of color within the globs by documenting the color preferences of sequentially encountered neurons along microelectrode penetrations targeted to globs. We find that glob cells are clustered by color preference, suggesting that the globs are organized in color columns.

Results

Color-biased regions in PIT were identified using fMRI as described previously (7, 16). These globs are defined as those regions that show greater fMRI activation to equiluminant color stripes versus black-and-white stripes. Each glob is $\approx 1\text{--}3$ mm in diameter, encompassing hundreds of thousands of neurons. We examined the micro-organization of color-tuned neurons within the globs; specifically, we documented the relationship of the color tuning of adjacent neurons within the globs to test the hypothesis that the neurons are arranged in color columns. We made 34 electrode penetrations into globs, and recorded from a total of 315 units (range, 3–23 cells/penetration; mean, 9.7 ± 5.5 cells/penetration). We recorded from a total of 5 globs; each penetration was restricted to a single glob. On many occasions, pairs of neurons were recorded simultaneously at a given position along the electrode track, isolated with a dual-window discriminator, and distinguished based on waveform (see *Materials and Methods*).

Fig. 1 shows the responses of 6 single units located in fMRI-identified globs; each pair of recordings (A–C) was recorded along a single electrode penetration. The left panels in Fig. 1 A–C show poststimulus time histograms of the responses of a bar of optimal size and orientation to each of 135 different colors and black-and-white. The International Commission on Illumination (CIE) x and y coordinates for the colors are given

Author contributions: B.R.C. and D.Y.T. designed research; B.R.C. performed research; B.R.C. and D.Y.T. contributed new reagents/analytic tools; B.R.C. analyzed data; and B.R.C. wrote the paper.

The authors declare no conflict of interest.

This article is a PNAS Direct Submission.

¹To whom correspondence should be addressed. E-mail: bconway@wellesley.edu.

This article contains supporting information online at www.pnas.org/cgi/content/full/0810943106/DCSupplemental.

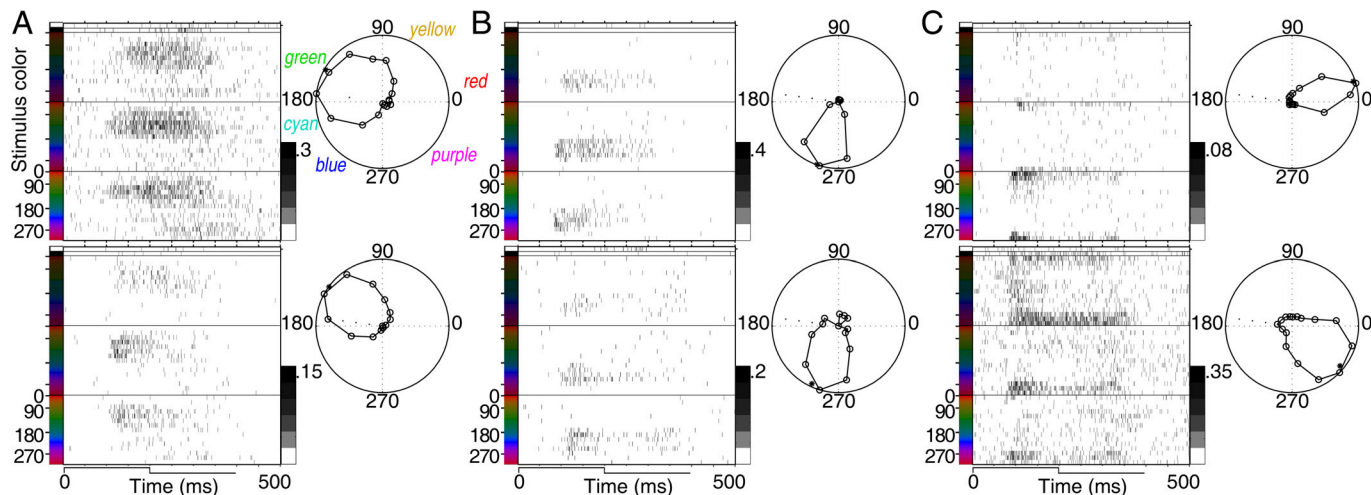


Fig. 1. Color-tuning of 6 glob cells. (A) A pair of green-tuned cells recorded simultaneously from a single electrode penetration. The panels on the left show poststimulus time histograms to an optimally shaped bar of various colors. Responses were determined to white and black (top 2 rows in each histogram) and to 3 sets of 45 colored versions of the bar presented against a neutral gray background. One set of colors was of lower luminance than the background (top section of each histogram), another set was equiluminant with the background (middle section), and a third set was of higher luminance than the background (bottom section). The CIELUV hue angles are given in degrees (see Table S1 and Fig. S2). For ease of presentation, the responses to each color set are compressed into 15 rows, with each row showing the average response to 3 consecutive colors in the cycle. The stimulus onset is at 0 ms. Stimulus duration is indicated by the step at the bottom (histogram bins, 1 ms). The gray scale bar shows the average number of spikes per stimulus repeat per bin. The lack of activity immediately following stimulus onset up to ≈ 70 ms is the response latency. The panel on the right shows the color tuning determined using a subset of stimuli that sampled the CIELUV color space at uniform color-angle intervals (see Materials and Methods); the peak is normalized to the maximum response. An asterisk indicates the Rayleigh vector. The P value of the Rayleigh vector is .02 for the top cell and .005 for the bottom cell, and the color-tuning index (CI, see Materials and Methods) is 0.93 for the top cell and 0.97 for the bottom cell. (B) A pair of blue-tuned cells recorded simultaneously from a single electrode penetration. The P value of the Rayleigh vector is .004 for the top cell and .04 for the bottom cell, and the CI is 0.96 for both cells. (C) A pair of cells tuned in the red region, recorded from a single electrode penetration, 175 μm apart. The P value of the Rayleigh vector is .03 for the top cell and .06 for the bottom cell, and the CI is 0.93 for the top cell and 0.97 for the bottom cell.

in supporting information (SI) Table S1. All of the cells whose responses are shown in Fig. 1 not only were significantly color-tuned, but also retained this color tuning across changes in luminance, a common feature of glob cells (7). Some 96% (303/312) of the recorded glob cells were color-tuned (Fig. S1), as determined by a significant Rayleigh vector length or a color index (CI) > 0.5 (see Materials and Methods).

The right panels in Fig. 1A–C show, as a polar plot, the relative magnitude of the response to a subset of colors that sample the CIELUV color space at uniform color-angle intervals (Fig. S2). This subset comprises 16 colors that were equiluminant with one another and with the neutral adapting gray background. All of the analyses in this report are restricted to data obtained in response to this restricted color set.

The 2 cells whose responses are shown in Fig. 1A had very similar color tuning but different temporal dynamics. The cell shown in the top panel gave a response that built up gradually following stimulus onset and was sustained throughout the stimulus presentation; the cell shown in the bottom panel gave a response that was more transient. These cells were recorded simultaneously and so were likely to be physically adjacent units. The cells whose responses are shown in Fig. 1B also were recorded simultaneously; they too had similar color tuning but different temporal dynamics. The cells shown in Fig. 1C were $\approx 175 \mu\text{m}$ apart; both were optimally sensitive to colors in the red region, although their peaks were separated by $\approx 60^\circ$.

The neurons of each pair shown in Fig. 1 had very similar color tuning, suggesting that similarly tuned neurons are clustered. Consistent with the organization of these clusters as columns, we found that the majority of neurons encountered along a long penetration roughly perpendicular to the cortical surface had similar color tuning. Fig. 2 shows the responses of all 22 cells encountered along a single deep penetration into a ventral glob. Fig. 2A shows a confirmational MRI image with the electrode

in place; the fMRI activity (equiluminant color $>$ black-and-white) is shown superimposed on the high-resolution anatomical MRI image. The electrode appears black on the MRI image, with its tip ending in the glob. The inset shows a line drawing of an enlargement of the white-boxed region, indicating the relationship between the vertical electrode penetration and the contour of the cortex. Most of the neurons (19/22) in this penetration had color tuning within the red region of the CIELUV color space (Fig. 2B and C). On close inspection, the electrode was not perfectly vertical relative to the thickness of the cortical sheet, but slightly oblique (angle θ in Fig. 2A). Correspondingly, the color tuning was not exactly the same at all positions along the electrode trajectory, but progressed gradually through perceptual color space from orange (80°), through red (6°), to bluish-red (330°), a significant trend (correlation coefficient, $P < .01$). The 3 outliers along the penetration (gray symbols in Fig. 2C and D) had color tuning that was complementary to red (e.g., third cell in Fig. 2B). The outliers also had longer latencies than the remaining cells (Fig. 2D). Like the cells of the penetration shown in Fig. 2, the color preference of cells in most penetrations tended to cluster, and often shifted gradually from one cell to the next along any given electrode penetration (Fig. 3). Fig. 3 also shows that a single glob was not restricted to cells of a single color preference.

We used 2 analyses to quantitatively test the hypothesis that color-tuned neurons are clustered. First, we plotted the color preference of each cell as a function of the color preference of its neighbor ($n = 284$ pairs; Fig. 4). The axes of Fig. 4 are translations of circular axes (the circumference of the polar plots in Fig. 1). The axes extend more than 360° to accommodate those neuron pairs that spanned 0° . (If the axes were not extended, then a pair of neurons preferring 7° and 341° would not reside close to the diagonal, even though the difference in peak color tuning is only 26° .) No pair of cells is plotted twice. The data points in Fig. 4A,

suggest that the transitions are gradual, leaving open the possibility that the columns are arranged according to a chromotopic map. Consistent with this idea, we found that the tuning of sequentially encountered neurons along a few electrode penetrations shifted gradually through small sections of the perceptual color space (red–orange–yellow–green–blue–purple–red; Figs. 2 and 3), although no penetration spanned the entire color space. In any event, the scale of the clusters is at least an order of magnitude smaller than the scale of the globs, so there is sufficient space within a single glob for a complete complement of color columns to represent all of color space, prompting us to wonder whether each glob functions as a color “hypercolumn.”

Materials and Methods

All animal procedures were performed in accordance with the National Institutes of Health’s Guide for Care and Use of Laboratory Animals, regulations for the welfare of experimental animals issued by the Federal Government of Germany, and stipulations of Bremen authorities.

Functional Magnetic Resonance Imaging. Experimental procedures for fMRI in alert macaques are available elsewhere (22, 35). Globs were identified using procedures described previously (7). Two macaque monkeys were trained for a juice reward to fixate a visual display while the animals were situated in a chair fit for a Siemens 3T horizontal-bore scanner. Red and blue equiluminant and achromatic gratings (0.29 cycle/degree, drifting at 0.29 cycle/s, alternating direction every 2 s) were displayed with an LCD projector in separate blocks interleaved with blocks of uniform gray, maintaining a constant mean luminance of 19.3 cd/m². Luminance was measured with a Minolta CS-100 chromometer. The minimal response of area MT was used to determine which stimuli were functionally equiluminant (16). The equiluminant stimulus had an L-cone contrast of 0.33, an M-cone contrast of 0.38, and an S-cone contrast of 0.98, where L-cone contrast = $(L_{red} - L_{blue}) / (L_{red} + L_{blue})$, with L_{red} the L activity elicited by the red phase of the stimulus and L_{blue} the L activity elicited by the blue phase (36). fMRI requires extensive signal averaging, limiting the number of stimulus dimensions that we could test. For the fMRI color stimulus, we chose to use a red-blue grating, which would be expected to activate both chromatic cardinal axes and a majority of the cone-opponent neurons in early visual areas. We chose the particular spatial frequency because it would be expected to activate the relatively coarse receptive fields of color neurons in earlier visual areas, which serve as the inputs to the brain region investigated in this work.

Scanning was done using an i.v. contrast agent, ferumoxtran-10 (Sinerem, Guerbet, France; concentration 21 mg Fe/mL in saline, 8 mg Fe/kg). The voxel size was 1.25 mm³ for most experiments and 1.5 mm³ in a few, yielding qualitatively similar results. The spatial distribution of globs has been shown previously (7), along with the specific globs that were targeted for the single-unit experiments described here (Fig. 3). Fixation was continuously monitored during all experiments using an ISCAN infrared eye monitor (ISCAN, Burlington, MA), and monkeys were rewarded only for maintaining constant fixation. Data analysis was performed using FREESURFER software (<http://surfer.nmr.mgh.harvard.edu/>). Data were motion-corrected with the AFNI motion-correction algorithm and intensity-normalized (35).

Single-Unit Recording. Detailed methods for single-unit recording in alert macaques have been given elsewhere (21, 37), as has the method for targeting the globs (7). A total of 23 penetrations targeting globs were used in 1 animal, and 10 penetrations were used in a second animal. An additional penetration (2 cells) was made into the anterior wall of the lunate sulcus of a third animal at the location of a putative glob, although a confirmational MRI was not done. Single-unit responses were measured in alert fixating animals using routine electrophysiological recording apparatus (BAK Electronics, Mount Airy, MD) and tungsten microelectrodes (12–18 m Ω) coated with an insulation film sparing the tip (FHC, Brunswick, ME) (38). Precise electrode depths were maintained using an oil hydraulic microdrive (Narishige). The initial entrance of the electrode into the brain, the depth of any white matter–gray matter junctions, and any exits and reentrances of an electrode passing through a sulcus were documented. The mean penetration length measured from the first glob cell encountered to the last one recorded in a given penetration was $41 \pm 35 \mu\text{m}$ (range, 0–880 μm). An attempt was made to record from every neuron encountered along an electrode path, which constrained the length of the penetrations. A total of 284 pairs of adjacent cells were recorded (Fig. 4A and B). Up to 2 neurons were isolated from a given depth of recording. “Adjacent cell” was defined as either a simultaneously recorded cell or the

next cell recorded after advancement of the electrode following a recording of a cell. The majority of adjacent cells (180/284) were recorded at a $< 25\text{-}\mu\text{m}$ separation distance along the electrode track; 218/284 were recorded at a $< 100\text{-}\mu\text{m}$ separation distance, and 260/284 were recorded at a $< 200\text{-}\mu\text{m}$ separation distance. After numerous recording sessions, with the electrode still in position at the end of the penetration, the electrode was carefully glued to the plastic guide tube, and the electrode advancer was removed. The animal was transferred to the MRI scanner, and a high-resolution anatomical scan was made to confirm the location of the electrode (Fig. 2A).

To provide a common basis for comparing recordings across electrode penetrations, which entered the cortex at various angles, Fig. 5 defines the distance separating pairs of cells as the distance between the cells along the penetration projected on the flattened cortical sheet. This distance was determined using trigonometry after measuring the angle of the penetration relative to the cortical surface (using the MRI electrode confirmation) and the neuron depth. For example, in Fig. 2A, we measured θ from the MRI, and using the known electrode depth (“ y ”) we calculated the distance parallel to the cortical sheet (“ x ”) using $\sin(\theta)$. The electrode entered the cortex normal to the cortical sheet in the sagittal plane. In Fig. 5, neurons with separation distances between 0 and 0.05 mm are plotted at 0.05 mm, neurons with separation distances between 0.05 mm and 0.1 mm are plotted at 0.1 mm, and so on.

Color Tuning. Single-unit responses were measured as described previously (7). We used optimal stimulus dimensions (bar length, width, and position) for each cell, and then varied the color of the stimulus. The stimulus set comprised 135 colors, consisting of 3 sets of 45 colors, plus black and white. The colors within a set were equiluminant with one another, spanned the full color gamut of the monitor, and were as saturated as the monitor could produce (CIE x and y coordinates in Table S1). The colors of one set were brighter (7.8 cd/m²) than the background, those of another set were photometrically equiluminant with the background (3.05 cd/m²), and those of the third set were darker than the background (0.62 cd/m²). Responses to black (0.02 cd/m²) and white (78.2 cd/m²) were measured as well. All colors had color discernible to human observers. The 2 color sets of equal and higher luminance than the adapting background were vividly colored, photopic, and likely did not involve rods; stimuli of the lowest luminance set may be considered mesopic and to have involved rods, although these stimuli were surrounded by an adapting background that maintained photopic conditions.

The dimensions of perceptual color space are unsettled (30), so it is not clear what stimulus set would be appropriate for assaying color tuning. The stimulus set that we used was large enough so that we could select responses to a subset of stimuli to measure tuning defined by the human CIELUV color space, which is more or less uniform. The stimuli of this “CIELUV subset” were all equiluminant with one another and with the background, and the CIELUV color space was sampled at uniform color-angle intervals (Fig. S2; Table S1). All of the analysis in this work is restricted to responses to this subset of stimuli, but the conclusions are not affected if the entire stimulus set is included.

To obtain neural responses, the different colors were presented in pseudorandom order. Within the time frame in which the 135 colors were presented, black-and-white versions of the stimulus were each presented 3 times. Responses of a given cell were measured to multiple presentations of this cycle and averaged. Each stimulus was displayed for 200 ms and separated in time from the previous and subsequent stimuli by 200 ms, during which time the animal was rewarded for maintaining constant fixation. Every visually responsive cell was tested; a cell was included in the analysis if responses to at least 2 complete stimulus cycles were obtained. In most cases, the cell was held long enough to allow us to measure the responses to at least 5 stimulus cycles.

The response to each color was defined as the average response during a 200-ms window, corresponding to the duration of the stimulus, following the visual latency, defined as > 3 standard deviations above the background firing rate. Optimal color tuning in all analyses was defined as the stimulus of the CIELUV subset that elicited the maximum response. The tuning curves obtained by analyzing the responses to the CIELUV subset (e.g., polar plots in Figs. 1 and 2) were then interpolated every 11.25°, and the Rayleigh statistical test was performed (asterisks in Fig. 1 and Fig. S1). The length of the Rayleigh vector was defined as 1 minus the P value of the vector and thus varied from 0 (for circular distributions centered at the origin) to 1 (for highly asymmetric distributions reflecting maximal hue tuning). Color tuning also was assessed using a color-tuning index: $CI = [\text{maximum response to any color} - \text{maximum response to black or white}] / [\text{maximum response to any color} + \text{maximum response to black or white}]$. CI values of 0.5 indicate that the color response was 3 times the response to black or white; cells with a $CI \geq 0.5$ or significant Rayleigh vector lengths were considered color-tuned (Fig. S1). More than 96% of the recorded neurons were considered color-tuned; all cells (including the minority that were not color-tuned) were included in the analysis.

ACKNOWLEDGMENTS. We thank Nicole Schweers and Sebastian Moeller for technical assistance and Margaret Livingstone, David Hubel, and Thorsten Hansen for comments on the manuscript. We also thank Anya Hurlbert for her expert advice on color spaces and MATLAB code. This work was

funded by the Alexander von Humboldt Foundation, the German Ministry of Science (Grant 01GO0506, Bremen Center for Advanced Imaging), the Neuroscience Program, Wellesley College, and the Whitehall Foundation.

1. Horton JC, Adams DL (2005) The cortical column: A structure without a function. *Philos Trans R Soc Lond B Biol Sci* 360:837–862.
2. Hubel DH, Wiesel TN (1968) Receptive fields and functional architecture of monkey striate cortex. *J Physiol* 195:215–243.
3. Albright TD, Desimone R, Gross CG (1984) Columnar organization of directionally selective cells in visual area MT of the macaque. *J Neurophysiol* 51:16–31.
4. Adams DL, Zeki S (2001) Functional organization of macaque V3 for stereoscopic depth. *J Neurophysiol* 86:2195–2203.
5. Hubel DH, Wiesel TN (1974) Sequence regularity and geometry of orientation columns in the monkey striate cortex. *J Comp Neurol* 158:267–293.
6. Barlow HB (1986) Why have multiple cortical areas? *Vision Res* 26:81–90.
7. Conway BR, Moeller S, Tsao DY (2007) Specialized color modules in macaque extrastriate cortex. *Neuron* 56:560–573.
8. Livingstone MS, Hubel DH (1984) Anatomy and physiology of a color system in the primate visual cortex. *J Neurosci* 4:309–356.
9. Zeki S (1996) Are areas TEO and PIT of monkey visual cortex wholly distinct from the fourth visual complex (V4 complex)? *Proc R Soc London B Biol Sci* 263:1539–1544.
10. Shipp S, Zeki S (1995) Segregation and convergence of specialised pathways in macaque monkey visual cortex. *J Anat* 187:547–562.
11. Felleman DJ, Xiao Y, McClendon E (1997) Modular organization of occipito-temporal pathways: Cortical connections between visual area 4 and visual area 2 and posterior inferotemporal ventral area in macaque monkeys. *J Neurosci* 17:3185–3200.
12. Xiao Y, Zych A, Felleman DJ (1999) Segregation and convergence of functionally defined V2 thin stripe and interstripe compartment projections to area V4 of macaques. *Cereb Cortex* 9:792–804.
13. Zeki S (1980) The representation of colours in the cerebral cortex. *Nature* 284:412–418.
14. Stoughton CM, Conway BR (2008) Neural basis for unique hues. *Curr Biol* 18:R698–R699.
15. Zeki SM (1973) Colour coding in rhesus monkey prestriate cortex. *Brain Res* 53:422–427.
16. Conway BR, Tsao DY (2006) Color architecture in alert macaque cortex revealed by fMRI. *Cereb Cortex* 16:1604–1613.
17. Gegenfurtner KR (2003) Cortical mechanisms of colour vision. *Nat Rev Neurosci* 4:563–572.
18. LeVay S, Voigt T (1988). Ocular dominance and disparity coding in cat visual cortex. *Vis Neurosci* 1:395–414.
19. Conway BR (2009) Color vision, cones, and color-coding in the cortex. *Neuroscientist* 15:274–290.
20. Rushton WA (1972) Pigments and signals in colour vision. *J Physiol* 220:1P–31P.
21. Conway BR (2001) Spatial structure of cone inputs to color cells in alert macaque primary visual cortex (V-1). *J Neurosci* 21:2768–2783.
22. Conway BR, Livingstone MS (2006) Spatial and temporal properties of cone signals in alert macaque primary visual cortex. *J Neurosci* 26:10826–10846.
23. Wachtler T, Sejnowski TJ, Albright TD (2003) Representation of color stimuli in awake macaque primary visual cortex. *Neuron* 37:681–691.
24. Horwitz GD, Chichilnisky EJ, Albright TD (2007) Cone inputs to simple and complex cells in V1 of awake macaque. *J Neurophysiol* 97:3070–3081.
25. Hubel DH, Livingstone MS (1987) Segregation of form, color, and stereopsis in primate area 18. *J Neurosci* 7:3378–3415.
26. Xiao Y, Wang Y, Felleman DJ (2003) A spatially organized representation of colour in macaque cortical area V2. *Nature* 421:535–539.
27. Kiper DC, Fenstemaker SB, Gegenfurtner KR (1997) Chromatic properties of neurons in macaque area V2. *Vis Neurosci* 14:1061–1072.
28. Komatsu H, Ideura Y, Kaji S, Yamane S (1992) Color selectivity of neurons in the inferior temporal cortex of the awake macaque monkey. *J Neurosci* 12:408–424.
29. Koida K, Komatsu H (2007) Effects of task demands on the responses of color-selective neurons in the inferior temporal cortex. *Nat Neurosci* 10:108–116.
30. Conway BR, Stoughton CM (2009) Towards a neural representation for unique hues. *Curr Biol* 19:R442–R443.
31. Mollon JD (2009) A neural basis for unique hues? *Curr Biol* 19:R441–R443.
32. Murphey DK, Yoshor D, Beauchamp MS (2008) Perception matches selectivity in the human anterior color center. *Curr Biol* 18:216–220.
33. Kusunoki M, Moutoussis K, Zeki S (2006) Effect of background colors on the tuning of color-selective cells in monkey area V4. *J Neurophysiol* 95:3047–3059.
34. Cowey A (1979) Cortical maps and visual perception: The Grindley Memorial Lecture. *Q J Exp Psychol* 31:1–17.
35. Tsao DYFW, Knutsen TA, Mandeville JB, Tootell RBH (2003) Faces and objects in macaque cerebral cortex. *Nat Neurosci* 6:989–995.
36. Stockman A, Sharpe LT, Merbs S, Nathans J (2000) Spectral sensitivities of human cone visual pigments determined in vivo and in vitro. *Methods Enzymol* 316:626–650.
37. Livingstone MS (1998) Mechanisms of direction selectivity in macaque V1. *Neuron* 20:509–526.
38. Hubel DH (1957) Tungsten microelectrode for recording from single units. *Science* 125:549–550.